

Supersensitive sensing of quantum reservoirs via breaking antisymmetric coupling

Ji-Bing Yuan^{*},¹ Zhi-Min Tang,¹ Ya-Ju Song,¹ Shi-Qing Tang,¹ Zhao-Hui Peng,² Xin-Wen Wang[†],¹ and Le-Man Kuang^{‡3,4}

¹*Key Laboratory of Opto-electronic Control and Detection Technology of University of Hunan Province, and College of Physics and Electronic Engineering, Hengyang Normal University, Hengyang 421002, China*

²*Hunan Provincial Key Laboratory of Intelligent Sensors and Advanced Sensor Materials, and Department of Physics, Hunan University of Science and Technology, Xiangtan 411201, China*

³*Key Laboratory of Low-Dimensional Quantum Structures and Quantum Control of Ministry of Education, and Department of Physics, Hunan Normal University, Changsha 410081, China*

⁴*Synergetic Innovation Academy for Quantum Science and Technology, Zhengzhou University of Light Industry, Zhengzhou 450002, China*

(Dated: October 20, 2023)

We investigate the utilization of a single generalized dephasing qubit for sensing a quantum reservoir, where the antisymmetric coupling between the qubit and its reservoir is broken. It is found that in addition to the decay factor encoding channel, the antisymmetric coupling breaking gives rise to another phase factor encoding channel. We introduce an optimal measurement for the generalized dephasing qubit which enables the practical measurement precision to reach the theoretical ultimate precision quantified by the quantum signal-to-noise ratio (QSNR). As an example, the generalized dephasing qubit is employed to estimate the *s*-wave scattering length of an atomic Bose-Einstein condensate. It is found that the phase-induced QSNR caused by the antisymmetric coupling breaking is at least two orders of magnitude higher than the decay-induced QSNR at the millisecond timescale and the optimal relative error can achieve a scaling $\propto 1/t$ with t being the encoding time in long-term encoding. Our work opens a way for supersensitive sensing of quantum reservoirs.

I. INTRODUCTION

Any realistic quantum systems inevitably interact with their surrounding quantum reservoirs, and undergo quantum decoherence [1]. It is important to access and characterize the quantum reservoirs, both in theoretical researches and practical applications such as quantum coherence protection [2, 3] and reservoir engineering [4, 5]. However, for a complex quantum reservoir with large number of degrees of freedom, it is a difficulty to precisely estimate various parameters that characterize the quantum reservoir. An effective way to overcome this difficulty is using quantum probes [6–15]. A quantum probe is a small and controllable quantum system which is prepared in a proper initial state. When the quantum probe interacts with the quantum reservoir interested, quantum correlations between them will be generated, which make the probe become sensitive to the fluctuations of the reservoir. Information of the parameter to be estimated from the reservoir may be extracted by performing suitable measurement on the probe, whose precision of estimation has been widely studied using the tools of quantum estimation theory [16, 17]. As restricted by the quantum Cramér-Rao (QCR) bound, ultimate precision of any estimation procedure can be quantified by means of quantum Fisher information (QFI) or the corresponding dimensionless quantum signal-to-noise ratio (QSNR) [18, 19]. The larger QFI (QSNR) indicates the better estimation strategy.

As the simplest quantum probe, a single qubit (referred to as a two-level system) to estimate parameters of a quantum

reservoir has attracted significant attention [20–28]. It is well-known that the relaxation timescales are much longer than the dephasing timescales in the qubit decoherence process [1, 29]. Therefore, if the parameter estimation time is relatively short, it is reasonable that employing pure dephasing model to describe the interaction between the qubit probe and the reservoir in the estimation process. As a matter of fact, the pure dephasing model has been widely applied to detect various properties of reservoirs such as measuring ultra-low temperatures [30–34], probing the cutoff frequency of Ohmic reservoirs [35–39], estimating various coupling strengths [38–40], and detecting the non-Markovian properties [41–43]. The interaction Hamiltonian in the dephasing model of a single qubit is usually taken to be [1]

$$\hat{H}_I = \hat{\sigma}_z \sum_{\mathbf{k}} (g_{\mathbf{k}} \hat{b}_{\mathbf{k}}^\dagger + g_{\mathbf{k}}^* \hat{b}_{\mathbf{k}}), \quad (1)$$

where $\hat{\sigma}_z = |1\rangle\langle 1| - |0\rangle\langle 0|$ is the Pauli operator with $|1\rangle$ ($|0\rangle$) being upper (lower) energy level of the qubit probe, $\hat{b}_{\mathbf{k}}(\hat{b}_{\mathbf{k}}^\dagger)$ represents bosonic annihilation (creation) operator for the k -th reservoir mode and $g_{\mathbf{k}}$ is coupling strength. It should be stressed that the coupling form in Eq. (1) has antisymmetry, with the qubit in the lower energy level having an opposite coupling strength with each mode of the reservoir compared to the qubit in the upper energy level. We notice that this antisymmetric coupling only allows the reservoir's parameter information to be encoded into the qubit's decay factor, resulting in a degradation of sensing precision over time during extended encoding [44].

In this paper, to fully exploit the potential of a single dephasing qubit in estimating quantum reservoir's parameters, we break the antisymmetry of the coupling in Eq. (1) and assume that the qubit in each energy level couples with each mode of the reservoir with arbitrary coupling strength. During the encoding process, we find that in addition to the decay

^{*}Email: jbyuan@hynu.edu.cn

[†]Email: xwwang@hynu.edu.cn

[‡]Email: lmkuang@hunnu.edu.cn

factor encoding channel, this antisymmetric coupling breaking leads to the reservoir's parameters information being encoded into the qubit's phase factor. Therefore, the QFI for a certain reservoir's parameter in the generalized dephasing model is composed of two parts: one part is the decay-induced QFI, and the other part is the phase-induced QFI. This implies that antisymmetric coupling breaking may improve the estimation precision of a single dephasing qubit for estimating reservoir's parameters. Moreover, a practical measurement scheme is proposed that enables the sensitivity of the generalized dephasing qubit to saturate the QCR bound.

To show the advantages of using the generalized dephasing qubit for sensing quantum reservoirs, we propose a system of an impurity qubit immersed in an atomic Bose-Einstein condensate (BEC) to simulate the generalized dephasing model and use the dephasing qubit to estimate the *s*-wave scattering length of the BEC, which is an important parameter in ultracold gases [45]. To quantify the sensing precision independently of its values, the dimensionless QSNR is used instead of QFI for consideration. We study the dynamical behaviors of the decay-induced QSNR and the phase-induced QSNR separately. It is found that the phase-induced QSNR caused by the antisymmetric coupling breaking is at least two orders of magnitude higher than the decay-induced QSNR at the millisecond timescale. Furthermore, the optimal relative error can achieve a scaling $\propto 1/t$ in long-term encoding, which implies that the antisymmetric coupling breaking allows the encoding time t to be utilized as a resource for enhancing the sensing precision. Therefore, one can say that antisymmetric coupling breaking makes it possible to achieve supersensitive sensing of quantum reservoirs by the single generalized dephasing qubit.

II. THE GENERALIZED DEPHASING MODEL

The Hamiltonian of the generalized dephasing model in this paper is given as

$$\hat{H} = \frac{\omega_0}{2} \hat{\sigma}_z + \sum_{\mathbf{k}} \omega_{\mathbf{k}} \hat{b}_{\mathbf{k}}^\dagger \hat{b}_{\mathbf{k}} + \sum_{i=0,1} |i\rangle\langle i| \sum_{\mathbf{k}} (g_{\mathbf{k}i} \hat{b}_{\mathbf{k}}^\dagger + g_{\mathbf{k}i}^* \hat{b}_{\mathbf{k}}), \quad (2)$$

where ω_0 is level splitting between the lower energy ($|0\rangle$) and upper energy ($|1\rangle$) states, bosonic annihilation operator $\hat{b}_{\mathbf{k}}$ and creation operator $\hat{b}_{\mathbf{k}}^\dagger$ for mode \mathbf{k} satisfy the commutation relation $[\hat{b}_{\mathbf{k}}, \hat{b}_{\mathbf{k}}^\dagger] = 1$, $\omega_{\mathbf{k}}$ is the frequency of the k -th mode. The third term on the right side of the above equation is the interaction Hamiltonian, where $g_{\mathbf{k}0(1)}$ is the coupling strength between the qubit in state $|0\rangle$ ($|1\rangle$) and the k -th reservoir mode. Hereafter we set $\hbar = 1$.

Using the relations $|1\rangle\langle 1| = (I + \hat{\sigma}_z)/2$ and $|0\rangle\langle 0| = (I - \hat{\sigma}_z)/2$ and omitting the constant term, the interaction Hamiltonian

$$\hat{H}_I = \sum_{i=0,1} |i\rangle\langle i| \sum_{\mathbf{k}} (g_{\mathbf{k}i} \hat{b}_{\mathbf{k}}^\dagger + g_{\mathbf{k}i}^* \hat{b}_{\mathbf{k}}) \quad (3)$$

is rewritten as

$$\hat{H}_I = \hat{\sigma}_z \sum_{\mathbf{k}} (g_{\mathbf{k}} \hat{b}_{\mathbf{k}}^\dagger + g_{\mathbf{k}}^* \hat{b}_{\mathbf{k}}) + \sum_{\mathbf{k}} (\xi_{\mathbf{k}} \hat{b}_{\mathbf{k}}^\dagger + \xi_{\mathbf{k}}^* \hat{b}_{\mathbf{k}}), \quad (4)$$

where $g_{\mathbf{k}}$ is coupling strength between the Pauli operator $\hat{\sigma}_z$ of the qubit and the k -th reservoir mode and $\xi_{\mathbf{k}}$ is the amplitude of the k -th harmonic oscillator displacement (HOD). Between $g_{\mathbf{k}}$, $\xi_{\mathbf{k}}$ and $g_{\mathbf{k}0}$, $g_{\mathbf{k}1}$, there are following relationships

$$g_{\mathbf{k}} = \frac{g_{\mathbf{k}1} - g_{\mathbf{k}0}}{2}, \quad (5a)$$

$$\xi_{\mathbf{k}} = \frac{g_{\mathbf{k}1} + g_{\mathbf{k}0}}{2}. \quad (5b)$$

It is clearly observed from Eq. (5b) that setting $g_{\mathbf{k}0} = -g_{\mathbf{k}1}$ for all modes will cause the interaction Hamiltonian (4) to degenerate into the interaction Hamiltonian (1). In this paper, the coupling of the qubit in the lower energy level having an opposite coupling strength with each mode of the reservoir compared to the qubit in the upper energy level, i.e., $g_{\mathbf{k}0} = -g_{\mathbf{k}1}$ is referred to as antisymmetric coupling. In the generalized dephasing model we consider, the antisymmetric coupling is broken ($g_{\mathbf{k}0} \neq -g_{\mathbf{k}1}$), resulting in an extra HOD term which is the second term on the right side of the Eq. (4).

Next, we investigate how the quantum state of the qubit evolves over time under the generalized dephasing model. The initial state of the whole system is assumed to be a product state

$$\hat{\rho}_{tot}(0) = \hat{\rho}_s(0) \otimes \hat{\rho}_B(0), \quad (6)$$

where $\hat{\rho}_s(0) = |\psi\rangle\langle\psi|$ with $|\psi\rangle = 1/\sqrt{2}(|0\rangle + |1\rangle)$ is a pure state of the probe and $\hat{\rho}_B(0) = \prod_{\mathbf{k}} (1 - e^{\beta\omega_{\mathbf{k}}}) e^{-\beta\omega_{\mathbf{k}}\hat{b}_{\mathbf{k}}^\dagger\hat{b}_{\mathbf{k}}}$ is a thermal state of the reservoir, where $\beta = 1/k_B T$ with T and k_B being the temperature and the Boltzmann constant. Then the evolution state of the qubit probe is given as

$$\hat{\rho}_s(t) = \frac{1}{2} \begin{pmatrix} 1 & e^{-i\Phi(t)} e^{-\Gamma(t)} \\ e^{i\Phi(t)} e^{-\Gamma(t)} & 1 \end{pmatrix}, \quad (7)$$

where the decay factor $\Gamma(t)$ is

$$\Gamma(t) = \sum_{\mathbf{k}} 4|g_{\mathbf{k}}|^2 \frac{(1 - \cos \omega_{\mathbf{k}t})}{\omega_{\mathbf{k}}^2} \coth\left(\frac{\beta\omega_{\mathbf{k}}}{2}\right), \quad (8)$$

and the phase factor $\Phi(t)$ has following expression

$$\Phi(t) = \omega_0 t - \sum_{\mathbf{k}} 4\text{Re}\left[\frac{\xi_{\mathbf{k}} g_{\mathbf{k}}^*}{\omega_{\mathbf{k}}}\right] t + \sum_{\mathbf{k}} 4\text{Im}\left[\frac{\xi_{\mathbf{k}} g_{\mathbf{k}}^*}{\omega_{\mathbf{k}}^2} (1 - e^{-i\omega_{\mathbf{k}t}})\right]. \quad (9)$$

The detailed derivation of the evolution state $\hat{\rho}_s(t)$ in Eq. (7) can be found in Appendix A. We can see that in the generalized dephasing model, the reservoir's parameter information can be encoded both in the decay factor (8) and in the phase factor (9). For the dephasing model with antisymmetric coupling which is commonly employed in the study of quantum sensing of reservoirs, the reservoir's parameter information can only be encoded into the decay factor, due to the absence of HOD term ($\xi_{\mathbf{k}} = 0$). This can also be said that the breaking of antisymmetric coupling in the generalized dephasing model adds an additional encoding channel of phase factor.

III. OPTIMAL MEASUREMENT FOR THE GENERALIZED DEPHASING MODEL

In quantum parameter estimation theory, the estimation precision of a parameter λ of interest is restricted to the QCR bound

$$\delta\lambda \geq \frac{1}{\sqrt{v\mathcal{F}_\lambda^Q}}, \quad (10)$$

where $\delta\lambda$ is the mean square error, v represents the number of repeated experiments and \mathcal{F}_λ^Q denotes QFI with respect to the parameter λ . The QFI represents theoretically ultimate precision for single measurement, which can be obtained from the quantum state of the system, and more specifically from its eigenvalues and eigenvectors. Any qubit state in the Bloch sphere representation can be written as $\hat{\rho} = 1/2(\hat{I} + \mathbf{w} \cdot \hat{\sigma})$, where \hat{I} is 2×2 identity matrix, $\mathbf{w} = (w_x, w_y, w_z)^T$ is the real Bloch vector and $\hat{\sigma} = (\hat{\sigma}_x, \hat{\sigma}_y, \hat{\sigma}_z)$ represents the pauli matrices. The eigenvalues of the density operator ρ can be given as $(1 \pm w)/2$, where w is the length of the Bloch vector. The length $w = 1$ for pure state and $w < 1$ for mixed state. In the Bloch sphere representation the QFI with respect to the estimated parameter λ can be given as follows [18, 19]

$$\mathcal{F}_\lambda^Q = \begin{cases} |\partial_\lambda \mathbf{w}|^2, & w = 1; \\ |\partial_\lambda \mathbf{w}|^2 + \frac{(\mathbf{w} \cdot \partial_\lambda \mathbf{w})^2}{1-w^2}, & w < 1. \end{cases} \quad (11)$$

where ∂_λ denotes the derivative with respect to the estimated parameter λ . Therefore, to obtain the QFI of the evolution state $\hat{\rho}_S(t)$ in Eq. (7), we rewritten the evolution state as

$$\hat{\rho}_S(t) = \frac{1}{2}(\hat{I} + \mathbf{w} \cdot \hat{\sigma}), \quad (12)$$

where the Bloch vector is

$$\mathbf{w} = (\cos \Phi e^{-\Gamma}, \sin \Phi e^{-\Gamma}, 0) \quad (13)$$

with the length $w = e^{-\Gamma}$. By substituting the Bloch vector in Eq. (13) into the Eq. (11), the concrete expression of the QFI of the evolution state in Eq. (7) is obtained

$$\mathcal{F}_\lambda^Q = \frac{(\partial_\lambda \Gamma)^2}{e^{2\Gamma} - 1} + e^{-2\Gamma} (\partial_\lambda \Phi)^2. \quad (14)$$

The QFI (14) contains of two terms. The first term is called decay-induced QFI and is labeled as

$$\mathcal{F}_\lambda^{\parallel} = \frac{(\partial_\lambda \Gamma)^2}{e^{2\Gamma} - 1}, \quad (15)$$

and the second term is called phase-induced QFI and is denoted as

$$\mathcal{F}_\lambda^{\perp} = e^{-2\Gamma} (\partial_\lambda \Phi)^2. \quad (16)$$

Now we introduce an optimal measurement for the generalized dephasing model, which enables the sensitivity of the

qubit sensor to saturate the QCR bound. For a two-level system, the Fisher information associated with the measurement can be presented as [30]

$$\mathcal{F}_\lambda = \frac{1}{\langle \Delta \hat{X}^2 \rangle} \left(\frac{\partial \langle \hat{X} \rangle}{\partial T} \right)^2, \quad (17)$$

where $\langle \hat{X} \rangle$ and $\langle \Delta \hat{X}^2 \rangle$ are mean and variance of the measured observable. For an unbiased estimator, the error obeys $\delta\lambda \geq 1/\sqrt{v\mathcal{F}_\lambda} \geq 1/\sqrt{v\mathcal{F}_\lambda^Q}$, which indicates the QFI is the upper bound of the Fisher information associated with the measurement \hat{X} , i.e.,

$$\mathcal{F}_\lambda^Q = \max_{\hat{X}} \mathcal{F}_\lambda(\hat{X}) = \mathcal{F}_\lambda(\hat{\Lambda}) \quad (18)$$

with $\hat{\Lambda}$ being the optimal measurement. Finding the optimal measurement $\hat{\Lambda}$ to spur practical precision to reach the theoretically ultimate precision is of particular importance and challenge in quantum metrology. For this reason, we introduce two measurements

$$\hat{\sigma}_{\parallel} = \cos \Phi \hat{\sigma}_x + \sin \Phi \hat{\sigma}_y, \quad (19a)$$

$$\hat{\sigma}_{\perp} = \cos \Phi \hat{\sigma}_y - \sin \Phi \hat{\sigma}_x, \quad (19b)$$

which are respectively parallel and perpendicular to the Bloch vector of $\hat{\rho}_S(t)$ due to $\text{Tr}[\hat{\sigma}_{\parallel} \hat{\rho}_S(t)] = w$ and $\text{Tr}[\hat{\sigma}_{\perp} \hat{\rho}_S(t)] = 0$. It can be proved

$$\mathcal{F}_\lambda(\hat{\sigma}_{\parallel}) = \mathcal{F}_\lambda^{\parallel}, \quad \mathcal{F}_\lambda(\hat{\sigma}_{\perp}) = \mathcal{F}_\lambda^{\perp}. \quad (20)$$

The detailed verification process can be found in Appendix B. The optimal measurement related with evolution state in Eq. (7) is defined as

$$\hat{\Lambda} = \cos \varphi \hat{\sigma}_{\parallel} + \sin \varphi \hat{\sigma}_{\perp}, \quad (21)$$

where the angle φ satisfies $\tan \varphi = w(1 - w^2) \partial_\lambda \Phi / \partial_\lambda w$. One can prove

$$\mathcal{F}_\lambda(\hat{\Lambda}) \equiv \mathcal{F}_\lambda^Q. \quad (22)$$

The detailed verification process can be found in Appendix B. Equation (22) demonstrates that the measurement $\hat{\Lambda}$ in Eq. (21) does be the optimal measurement which enables the sensitivity of the generalized dephasing qubit sensor to saturate the QCR bound.

IV. QUANTUM SENSING TO AN ATOMIC BOSE-EINSTEIN CONDENSATE

A. Quantum simulation of the generalized dephasing model

In this subsection we propose a system of an impurity qubit immersed in an atomic BEC to simulate the generalized dephasing model. We consider an impurity qubit is immersed in a three-dimensional homogeneous BEC. The qubit probe is confined in a harmonic trap $V_A(\mathbf{r}) = m_A \omega_A^2 r^2/2$ that is independent of the internal states, where m_A is the mass of the

impurity and ω_A is the trap frequency. For $\omega_A \gg k_B T$, the spatial wave function of the qubit is the ground state of $V_A(\mathbf{r})$, i.e., $\varphi_A(\mathbf{r}) = \pi^{-3/4} \ell_A^{-3/2} \exp[-r^2/(2\ell_A^2)]$ with $\ell_A = \sqrt{1/(m_A \omega_A)}$. The Hamiltonian of the qubit is

$$\hat{H}_A = \frac{\Omega_A}{2} \hat{\sigma}_z, \quad (23)$$

where Ω_A is level splitting between the lower ($|0\rangle$) and upper ($|1\rangle$) states. The Hamiltonian of the BEC is given as

$$\hat{H}_B = \int d\mathbf{r} \hat{\psi}^\dagger(\mathbf{r}) \left(-\frac{\hbar^2 \nabla^2}{2m_B} + V(\mathbf{r}) - \mu \right) \hat{\psi}(\mathbf{r}) + \frac{g_B}{2} \int d\mathbf{r} \hat{\psi}^\dagger(\mathbf{r}) \hat{\psi}^\dagger(\mathbf{r}) \hat{\psi}(\mathbf{r}) \hat{\psi}(\mathbf{r}), \quad (24)$$

where $\hat{\psi}(\mathbf{r})$ and $\hat{\psi}^\dagger(\mathbf{r})$ are field creation and annihilation operators, satisfying the bosonic commutative relations $[\hat{\psi}(\mathbf{r}), \hat{\psi}^\dagger(\mathbf{r}')] = \delta(\mathbf{r} - \mathbf{r}')$ and $[\hat{\psi}(\mathbf{r}), \hat{\psi}(\mathbf{r}')] = [\hat{\psi}^\dagger(\mathbf{r}), \hat{\psi}^\dagger(\mathbf{r}')] = 0$, μ is chemical potential, the contact interaction strength

$$g_B = \frac{4\pi a_B}{m_B} \quad (25)$$

with a_B being the *s*-wave scattering length between one condensate atom and another and m_B being the mass of the condensate atom. Here we consider $V(\mathbf{r})$ is a very shallow spherical harmonic potential that the condensate can be taken as a homogeneous condensate. Then the field operator can be written as

$$\hat{\psi}(\mathbf{r}) = \sqrt{n} + \delta\hat{\psi}(\mathbf{r}). \quad (26)$$

where n is the density of the condensed part and $\delta\hat{\psi}(\mathbf{r})$ is the field operator of small non-condensed part. One can expand $\delta\hat{\psi}(\mathbf{r})$ as plane waves and perform Bogoliubov transformation

$$\delta\hat{\psi}(\mathbf{r}) = \frac{1}{\sqrt{\mathcal{V}}} \sum_{\mathbf{k}} (u_{\mathbf{k}} \hat{b}_{\mathbf{k}} - v_{\mathbf{k}} \hat{b}_{-\mathbf{k}}^\dagger) e^{i\mathbf{k}\cdot\mathbf{r}}, \quad (27)$$

where \mathcal{V} is the volume of the BEC, $\hat{b}_{\mathbf{k}}(\hat{b}_{\mathbf{k}}^\dagger)$ is bosonic annihilation (creation) operator satisfying the bosonic commutative relations. Here $u_{\mathbf{k}}$ and $v_{\mathbf{k}}$ are Bogoliubov transformation coefficients with the forms $u_{\mathbf{k}} = 1/2(\sqrt{\omega_{\mathbf{k}}/E_{\mathbf{k}}} + \sqrt{E_{\mathbf{k}}/\omega_{\mathbf{k}}})$, $v_{\mathbf{k}} = 1/2(\sqrt{\omega_{\mathbf{k}}/E_{\mathbf{k}}} - \sqrt{E_{\mathbf{k}}/\omega_{\mathbf{k}}})$, where kinetic energy $E_{\mathbf{k}} = k^2/(2m_B)$ and Bogoliubov excitation energy $\omega_{\mathbf{k}}$ reads

$$\omega_{\mathbf{k}} = \sqrt{E_{\mathbf{k}}^2 + 2ng_B E_{\mathbf{k}}}. \quad (28)$$

By substituting Eqs. (26) and (27) into the Hamiltonian (24) and omitting the constant term, the third and forth order in $\delta\hat{\psi}(\mathbf{r})$, the Hamiltonian of the BEC is diagonalized as

$$\hat{H}_B = \sum_{\mathbf{k}} \omega_{\mathbf{k}} \hat{b}_{\mathbf{k}}^\dagger \hat{b}_{\mathbf{k}}. \quad (29)$$

Let us consider the interaction Hamiltonian between the qubit probe and the BEC. For the qubit-BEC coupling, we assume that the qubit undergoes spin-dependent *s*-wave collisions with the BEC. The qubit-BEC interaction Hamiltonian is represented as

$$\hat{H}_I = \left(\sum_{i=0,1} g_i |i\rangle \langle i| \right) \int d\mathbf{r} |\varphi_A(\mathbf{r})|^2 \hat{\psi}^\dagger(\mathbf{r}) \hat{\psi}(\mathbf{r}), \quad (30)$$

where

$$g_i = \frac{2\pi a_i}{m_{AB}} \quad (31)$$

is the coupling strength of the qubit-BEC interaction with a_i being the *s*-wave scattering length between one condensate atom and the impurity qubit in state $|i\rangle$ and m_{AB} being reduced mass $m_{AB} = m_A m_B / (m_A + m_B)$. Through these processes of substituting Eqs. (26) and (27) into the interaction Hamiltonian (30), rewriting the $|1\rangle\langle 1|$ as $(I + \hat{\sigma}_z)/2$ and $|0\rangle\langle 0|$ as $(I - \hat{\sigma}_z)/2$, and omitting the constant term and the second order in $\delta\hat{\psi}(\mathbf{r})$, we obtain

$$\hat{H}_I = \frac{\Delta}{2} \hat{\sigma}_z + \sigma_z \sum_{\mathbf{k}} g_{\mathbf{k}} (\hat{b}_{\mathbf{k}} + \hat{b}_{\mathbf{k}}^\dagger) + \sum_{\mathbf{k}} \xi_{\mathbf{k}} (\hat{b}_{\mathbf{k}} + \hat{b}_{\mathbf{k}}^\dagger), \quad (32)$$

where $\Delta = n(g_1 - g_2)$, the k -th coupling strength $g_{\mathbf{k}}$ and the k -th HOD amplitude $\xi_{\mathbf{k}}$ are given as

$$g_{\mathbf{k}} = \frac{\sqrt{n}(g_1 - g_0)}{\sqrt{\mathcal{V}}} \sqrt{\frac{E_{\mathbf{k}}}{\omega_{\mathbf{k}}}} e^{-\frac{k^2 \ell_A^2}{4}}, \quad (33a)$$

$$\xi_{\mathbf{k}} = \frac{\sqrt{n}(g_1 + g_0)}{\sqrt{\mathcal{V}}} \sqrt{\frac{E_{\mathbf{k}}}{\omega_{\mathbf{k}}}} e^{-\frac{k^2 \ell_A^2}{4}}. \quad (33b)$$

Let $\Omega_A + \Delta = \omega_0$, the total Hamiltonian is

$$\hat{H} = \frac{\omega_0}{2} \hat{\sigma}_z + \sum_{\mathbf{k}} \omega_{\mathbf{k}} \hat{b}_{\mathbf{k}}^\dagger \hat{b}_{\mathbf{k}} + \sigma_z \sum_{\mathbf{k}} g_{\mathbf{k}} (\hat{b}_{\mathbf{k}} + \hat{b}_{\mathbf{k}}^\dagger) + \sum_{\mathbf{k}} \xi_{\mathbf{k}} (\hat{b}_{\mathbf{k}} + \hat{b}_{\mathbf{k}}^\dagger), \quad (34)$$

which confirms that the system of an impurity qubit immersed in an atomic BEC does simulate the generalized dephasing model. It is emphasized that the ratio of the k -th HOD amplitude $\xi_{\mathbf{k}}$ in Eq. (33b) to the k -th coupling strength $g_{\mathbf{k}}$ in Eq. (33a) is a physical quantity that is independent of \mathbf{k} . We refer to this ratio as relative HOD χ with following form

$$\chi = \frac{\xi_{\mathbf{k}}}{g_{\mathbf{k}}} = \frac{a_1 + a_0}{a_1 - a_0}. \quad (35)$$

The above equation shows the relative HOD χ can be widely adjusted by changing the *s*-wave scattering lengths a_0 and a_1 via Feshbach resonance [46].

B. Estimating the *s*-wave scattering length a_B of the BEC

In this subsection, we will illustrate the benefits of the generalized dephasing model in quantum sensing of quantum reservoirs. As an example, the impurity qubit is employed to estimate the *s*-wave scattering length a_B of the BEC, which is an important parameter in ultracold gases [45]. The initial state of the impurity qubit and BEC is prepared to be the state in Eq. (6). Under the control of the Hamiltonian (34), the evolution state of the impurity qubit must be the state in Eq. (7). Substituting $g_{\mathbf{k}}$ in Eq. (33a) and $\xi_{\mathbf{k}}$ in Eq. (33b) into the decay factor in Eq. (8) and the phase factor in Eq. (9), then using the continuum limit $\sum_{\mathbf{k}} \rightarrow \frac{\mathcal{V}}{(2\pi)^3} \int_0^{2\pi} d\varphi \int_0^\pi \sin \theta d\theta \int_0^\infty k^2 dk$, we obtain the decay factor

$$\Gamma(t) = P \int_0^\infty k^2 \frac{E_{\mathbf{k}}(1 - \cos \omega_{\mathbf{k}} t)}{\omega_{\mathbf{k}}^3} e^{-\frac{k^2 \ell_A^2}{2}} dk, \quad (36)$$

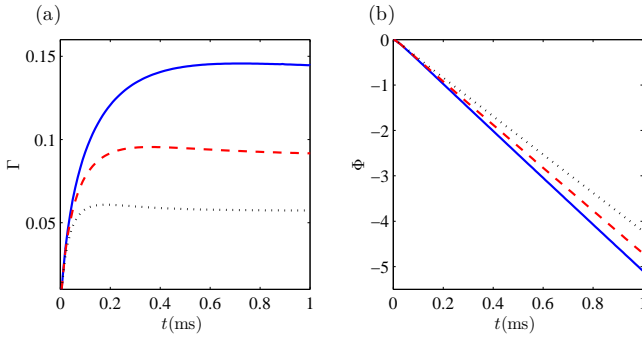


FIG. 1: (Color online) Dynamical behaviors of the decay factor Γ in (a) and the phase factor Φ in (b) for the s -wave scattering lengths $a_B = 0.5a_{Rb}$ (blue solid line), $a_B = a_{Rb}$ (red dashed line) and $a_B = 2a_{Rb}$ (black dotted line). The relative HOD is taken as $\chi = 1$.

and the phase factor

$$\Phi(t) = \chi P \int_0^\infty k^2 \frac{E_{\mathbf{k}}(\sin \omega_{\mathbf{k}} t - \omega_{\mathbf{k}} t)}{\omega_{\mathbf{k}}^3} e^{-\frac{k^2 \ell_A^2}{2}} dk, \quad (37)$$

where we consider zero temperature reservoir and the parameter $P = 2n(g_1 - g_0)^2/\pi^2$.

We give the reasonable values of parameters involved, before presenting numerical results based on the Eqs. (36) and (37). We consider a ^{23}Na impurity atom is immersed in a ^{87}Rb BEC with density $n = 10^{20}\text{m}^{-3}$. The impurity atom is trapped in an optical lattice with trapped characteristic length $\ell_A = 45\text{nm}$. The difference between the spin-dependent s -wave scattering lengths is taken to be $a_1 - a_0 = 2.9\text{nm}$. The s -wave scattering length a_B of the BEC is restricted by the condition $\sqrt{na_B^3} \ll 1$. As a consequence, the scattering length have to satisfy the inequality $a_B < 3a_{Rb}$, where $a_{Rb} = 5.3\text{nm}$ [41, 47].

Figures 1(a) and 1(b) depict the dynamical behaviors of the decay factor Γ and the phase factor Φ , respectively, for different s -wave scattering lengths $a_B = 0.5a_{Rb}$ (blue solid line), $a_B = a_{Rb}$ (red dashed line) and $a_B = 2a_{Rb}$ (black dotted line). As can be seen from Fig. 1(a), all decay factors for the three s -wave scattering lengths increase with time from zero and eventually reach different stationary values. This implies that the decay factor differences caused by changing the s -wave scattering length a_B tend to stabilize over time. And Fig. 1(b) shows that the phase factor differences caused by changing the s -wave scattering length a_B become larger with time.

To quantify the sensing precision of the s -wave scattering length a_B independently of its values, we introduce the dimensionless QSNR

$$Q_{a_B} = a_B^2 \mathcal{F}_{a_B}^Q, \quad (38)$$

and corresponding decay-induced QSNR $Q_{a_B}^{\parallel} = a_B^2 \mathcal{F}_{a_B}^{\parallel}$ and phase-induced QSNR $Q_{a_B}^{\perp} = a_B^2 \mathcal{F}_{a_B}^{\perp}$. From the QCR bound in Eq. (10), the optimal relative error and the QSNR has the relation

$$\frac{(\delta a_B)_{\min}}{a_B} = \frac{1}{\sqrt{\nu Q_{a_B}}}, \quad (39)$$

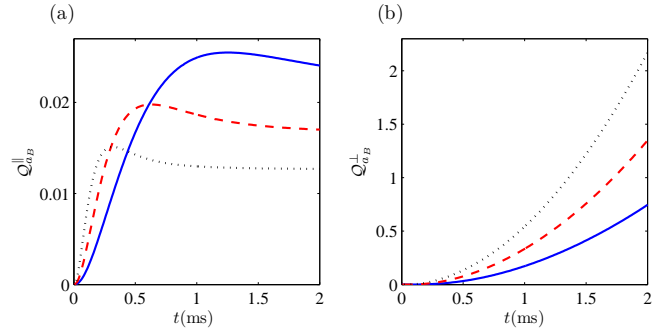


FIG. 2: (Color online) Time dependence of the decay-induced QSNR $Q_{a_B}^{\parallel}$ in (a) and phase-induced QSNR $Q_{a_B}^{\perp}$ in (b) for the s -wave scattering lengths $a_B = 0.5a_{Rb}$ (blue solid line), $a_B = a_{Rb}$ (red dashed line) and $a_B = 2a_{Rb}$ (black dotted line). The relative HOD is taken as $\chi = 1$.

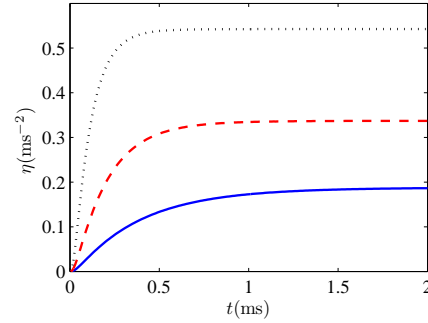


FIG. 3: (color online) The ratio η as a function of time t for the s -wave scattering lengths $a_B = 0.5a_{Rb}$ (blue solid line), $a_B = a_{Rb}$ (red dashed line) and $a_B = 2a_{Rb}$ (black dotted line).

which indicates the QSNR does quantify the ultimate precision of quantum sensing. Figures 2(a) and 2(b) plot dynamical behaviors of the decay-induced QSNR $Q_{a_B}^{\parallel}$ and phase-induced QSNR $Q_{a_B}^{\perp}$ for different s -wave scattering lengths $a_B = 0.5a_{Rb}$ (blue solid line), $a_B = a_{Rb}$ (red dashed line) and $a_B = 2a_{Rb}$ (black dotted line). All decay-induced QSNRs in Fig. 2(a) increase from zero to different steady values with time, while all phase-induced QSNRs in Fig. 2(b) increase continuously over time. In particular, it is observed that at the millisecond time scale, the phase-induced QSNR is at least two orders of magnitude higher than the decay-induced QSNR for the same s -wave scattering length a_B . This demonstrates that the phase factor encoding channel caused by the antisymmetric coupling breaking greatly enhances the ultimate precision of quantum sensing for the s -wave scattering length a_B .

To further explore the relationship of the phase-induced QSNR $Q_{a_B}^{\perp}$ with the encoding time t and the relative HOD χ , we define such a ratio

$$\eta = \frac{Q_{a_B}^{\perp}}{(\chi t)^2}. \quad (40)$$

Figure 3 presents the dynamical behaviors of the ratio in Eq. (40) for different s -wave scattering lengths $a_B = 0.5a_{Rb}$ (blue solid line), $a_B = a_{Rb}$ (red dashed line) and $a_B = 2a_{Rb}$

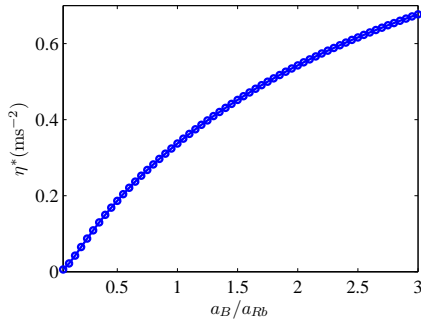


FIG. 4: (color online) The optimal ratio η^* as a function of the dimensionless s -wave scattering length of the BEC a_B/a_{Rb} .

(black dotted line). We can see that all the ratios for the three s -wave scattering lengths increase with time to different stable values and the ratio corresponding to a smaller s -wave scattering length a_B has a smaller stable value. In fact, such similar dynamical behaviors are still presented for other s -wave scattering lengths. This implies that there exists an optimal ratio η^* that is independent of the encoding time t and positively correlated with the s -wave scattering length a_B in long-term encoding. The functional relationship between the optimal ratio η^* and the dimensionless s -wave scattering length a_B/a_{Rb} is given in Fig. 4. It is shown that the optimal ratio η^* increases as increasing the s -wave scattering length a_B .

In long-term encoding, due to $Q_{a_B}^\perp \gg Q_{a_B}^\parallel$, the QSNR Q_{a_B} can be approximated as

$$Q_{a_B} \approx Q_{a_B}^\perp = \eta^*(\chi t)^2, \quad (41)$$

thus the optimal relative error has following simple expression

$$\frac{(\delta a_B)_{\min}}{a_B} = \frac{1}{\sqrt{\eta^* \chi t}}. \quad (42)$$

Equation (42) shows that encoding time t is a resource to enhance the ultimate precision of quantum sensing for the s -wave scattering length a_B , and that increasing the relative HOD χ in Eq. (35) can also improve the ultimate precision.

V. CONCLUSION

In conclusion, we studied the use of a single generalized dephasing qubit to perform quantum sensing of a quantum reservoir. In the generalized dephasing model, the antisymmetric coupling between the qubit and its reservoir is broken. It was found that in addition to the decay factor encoding channel, the antisymmetric coupling breaking gives rise to another encoding channel, namely the phase factor encoding channel. We used the QFI to quantify the ultimate precision of quantum

sensing and found that the QFI about the generalized dephasing qubit consists of the decay-induced QFI and the phase-induced QFI. We also introduced an optimal measurement for the generalized dephasing qubit which enables the practical measurement precision to reach the theoretical ultimate precision.

To show the advantages of using the generalized dephasing qubit for sensing quantum reservoirs, we proposed a system of an impurity qubit immersed in an atomic BEC to simulate the generalized dephasing model and employed the impurity qubit to estimate the s -wave scattering length of the BEC. To quantify the sensing precision independently of its values, the dimensionless QSNR was used instead of QFI for consideration. The dynamical behaviors of the decay-induced QSNR and the phase-induced QSNR were studied separately. It was found that the phase-induced QSNR is at least two orders of magnitude higher than the decay-induced QSNR at the millisecond timescale, and the phase-induced QSNR increases continuously over time, while the decay-induced QSNR remains constant in long-term encoding. Furthermore, it was discovered that the optimal relative error can achieve a scaling $\propto 1/(\chi t)$ during extended encoding. This means that extending the encoding time t and increasing the relative HOD χ can achieve supersensitive quantum sensing of the s -wave scattering length of the BEC.

The generalized dephasing model can also be well used for quantum sensing of other quantum reservoirs such as Ohmic-family reservoirs [35–39]. It is worth noting that the antisymmetric coupling breaking allows for the encoding of information about key parameters of the Ohmic-family spectral density such as the cutoff frequency and the reservoir coupling strength into the phase factor of the generalized dephasing qubit. Our work opens a way for supersensitive sensing of quantum reservoirs.

Acknowledgments

J. B. Yuan was supported by NSFC (No. 11905053), Scientific Research Fund of Hunan Provincial Education Department of China under Grant (No. 21B0647) and Hunan Provincial Natural Science Foundation of China under Grant (No. 2018JJ3006). Y. J. Song was supported by NSFC (No. 12205088). S. Q. Tang was supported by Scientific Research Fund of Hunan Provincial Education Department of China under Grant (No. 22A0507). Z. H. Peng was supported by NSFC (No. 11405052) and Hunan Provincial Natural Science Foundation of China under Grant (No. 2020JJ4286). L. M. Kuang was supported by NSFC (Nos. 12247105, 1217050862, and 11935006) and the science and technology innovation Program of Hunan Province (No. 2020RC4047).

Appendix A: derivation of evolution state of the qubit in the generalized dephasing model

We first introduce an unitary transformation

$$\hat{U} = \exp \left[\sum_{\mathbf{k}} \left(\hat{a}_{\mathbf{k}} \hat{b}_{\mathbf{k}}^\dagger - \hat{a}_{\mathbf{k}}^\dagger \hat{b}_{\mathbf{k}} \right) \right] \equiv \Pi_{\mathbf{k}} \hat{D}_{\mathbf{k}}(\hat{a}_{\mathbf{k}}), \quad (\text{A1})$$

where $\hat{D}_{\mathbf{k}}(\hat{a}_{\mathbf{k}}) = \exp \left[\left(\hat{a}_{\mathbf{k}} \hat{b}_{\mathbf{k}}^\dagger - \hat{a}_{\mathbf{k}}^\dagger \hat{b}_{\mathbf{k}} \right) \right]$ is generalized displace operator with

$$\hat{a}_{\mathbf{k}} = \frac{g_{\mathbf{k}} \hat{\sigma}_z + \xi_{\mathbf{k}}}{\omega_{\mathbf{k}}}. \quad (\text{A2})$$

Then we perform the unitary transformation on the Hamiltonian (2) of the main text and obtain

$$\hat{H}' = \hat{U} \hat{H} \hat{U}^\dagger = \frac{1}{2} \Delta \hat{\sigma}_z + \sum_{\mathbf{k}} \omega_{\mathbf{k}} \hat{b}_{\mathbf{k}}^\dagger \hat{b}_{\mathbf{k}}, \quad (\text{A3})$$

where

$$\Delta = \omega_0 - \sum_{\mathbf{k}} 4 \text{Re} \left[\frac{\xi_{\mathbf{k}} g_{\mathbf{k}}^*}{\omega_{\mathbf{k}}} \right]. \quad (\text{A4})$$

Here we omit the constant term and use the relation $\exp(\hat{A}) \hat{B} \exp(-\hat{A}) = \hat{B} + [\hat{A}, \hat{B}] + \frac{[\hat{A}, [\hat{A}, \hat{B}]]}{2!} + \dots$ to obtain the Hamiltonian (A3).

The evolution state of the qubit probe is represented as

$$\hat{\rho}_s(t) = \text{Tr}_B [e^{-i\hat{H}_B t} \hat{\rho}_s(0) \otimes \hat{\rho}_B(0) e^{i\hat{H}_B t}] \equiv \text{Tr}_B [\hat{U}^\dagger e^{-i\hat{H}' t} \hat{U} \hat{\rho}_s(0) \otimes \hat{\rho}_B(0) \hat{U}^\dagger e^{i\hat{H}' t} \hat{U}]. \quad (\text{A5})$$

According to the above equation, we can easily prove the diagonal elements unchanged. The off-diagonal elements are given as

$$\rho_{s,10}(t) = \rho_{s,01}(t)^* = \langle 1 | \hat{\rho}_s(t) | 0 \rangle = \frac{1}{2} e^{-i\Delta t} f_B(t). \quad (\text{A6})$$

Here $f_B(t)$ is a reservoir-dependent function with the following expression

$$f_B(t) = \prod_{\mathbf{k}} \text{Tr}_B [\hat{D}_{\mathbf{k}}^\dagger(\alpha_{\mathbf{k},0}) e^{i\omega_{\mathbf{k}} \hat{b}_{\mathbf{k}}^\dagger \hat{b}_{\mathbf{k}}} \hat{D}_{\mathbf{k}}(\alpha_{\mathbf{k},0}) \hat{D}_{\mathbf{k}}^\dagger(\alpha_{\mathbf{k},1}) e^{-i\omega_{\mathbf{k}} \hat{b}_{\mathbf{k}}^\dagger \hat{b}_{\mathbf{k}}} \hat{D}_{\mathbf{k}}(\alpha_{\mathbf{k},1}) \hat{\rho}_{B,\mathbf{k}}(0)], \quad (\text{A7})$$

where $\alpha_{\mathbf{k},1} = (\xi_{\mathbf{k}} + g_{\mathbf{k}})/\omega_{\mathbf{k}}$, $\alpha_{\mathbf{k},0} = (\xi_{\mathbf{k}} - g_{\mathbf{k}})/\omega_{\mathbf{k}}$ and $\hat{\rho}_{B,\mathbf{k}}(0)$ is a thermal state of the k -th mode. Using the following relations

$$\hat{D}(\alpha) \hat{D}(\beta) = \hat{D}(\alpha + \beta) \exp[i\text{Im}(\alpha\beta^*)], \quad \exp(x\hat{b}^\dagger \hat{b}) \hat{D}(\alpha) \exp(-x\hat{b}^\dagger \hat{b}) = \hat{D}(\alpha e^x), \quad (\text{A8})$$

we obtain

$$f_B(t) = e^{-i\Theta(t)} e^{-\Gamma(t)}, \quad (\text{A9})$$

where the decaying function is

$$\begin{aligned} e^{-\Gamma(t)} &= \prod_{\mathbf{k}} \text{Tr}_B \left[\hat{D}_{\mathbf{k}} \left[(\alpha_{\mathbf{k},1} - \alpha_{\mathbf{k},0})(1 - e^{i\omega_{\mathbf{k}} t}) \right] \hat{\rho}_{B,\mathbf{k}}(0) \right] \\ &= \exp \left[- \sum_{\mathbf{k}} 4|g_{\mathbf{k}}|^2 \frac{(1 - \cos \omega_{\mathbf{k}} t)}{\omega_{\mathbf{k}}^2} \coth \left(\frac{\beta \omega_{\mathbf{k}}}{2} \right) \right]. \end{aligned} \quad (\text{A10})$$

and the phase factor is given as

$$\begin{aligned} \Theta(t) &= \sum_{\mathbf{k}} \text{Im} \left[\alpha_{\mathbf{k},0} (\alpha_{\mathbf{k},0} - \alpha_{\mathbf{k},1})^* e^{-i\omega_{\mathbf{k}} t} + \alpha_{\mathbf{k},1}^* (\alpha_{\mathbf{k},1} - \alpha_{\mathbf{k},0}) e^{i\omega_{\mathbf{k}} t} + 2\alpha_{\mathbf{k},0} \alpha_{\mathbf{k},1}^* \right] \\ &= \sum_{\mathbf{k}} 4 \text{Im} \left[\frac{\xi_{\mathbf{k}} g_{\mathbf{k}}^*}{\omega_{\mathbf{k}}^2} \left(1 - e^{-i\omega_{\mathbf{k}} t} \right) \right]. \end{aligned} \quad (\text{A11})$$

Appendix B: derivation of the fisher information associated with the measurements

In this appendix, we calculate the fisher information associated with the measurements $\hat{\sigma}_{\parallel} = \cos \Phi \hat{\sigma}_x + \sin \Phi \hat{\sigma}_y$, $\hat{\sigma}_{\perp} = \cos \Phi \hat{\sigma}_y - \sin \Phi \hat{\sigma}_x$ and $\hat{\Lambda} = \cos \varphi \hat{\sigma}_{\parallel} + \sin \varphi \hat{\sigma}_{\perp}$, respectively. The evolution state in Eq. (7) of the main text is rewritten as

$$\hat{\rho}_S(t) = \frac{1}{2} (I + e^{-\Gamma(t)} \cos \Phi \hat{\sigma}_x + e^{-\Gamma(t)} \sin \Phi \hat{\sigma}_y). \quad (\text{B1})$$

Based on the above equation, we can obtain following relations

$$\begin{aligned} \langle \hat{\sigma}_{\parallel} \rangle &= w, & \langle \hat{\sigma}_{\perp} \rangle &= 0, & \langle \hat{\Lambda} \rangle &= \cos(\varphi)w, \\ \langle \hat{\sigma}_{\parallel}^2 \rangle &= \langle \hat{\sigma}_{\perp}^2 \rangle = \langle \hat{\Lambda}^2 \rangle = 1, & \langle \hat{\sigma}_{\perp} \hat{\sigma}_{\parallel} \rangle &= \langle \hat{\sigma}_{\parallel} \hat{\sigma}_{\perp} \rangle = 0. \end{aligned} \quad (\text{B2})$$

where the length of the Bloch vector $w = e^{-\Gamma}$.

(i) The fisher information associated with the measurement $\hat{\sigma}_{\parallel}$ is given as

$$\mathcal{F}_{\lambda}(\hat{\sigma}_{\parallel}) = \frac{(\partial_{\lambda} \langle \hat{\sigma}_{\parallel} \rangle)^2}{\langle \Delta \hat{\sigma}_{\parallel}^2 \rangle} = \frac{(\partial_{\lambda} w)^2}{1 - w^2} = \frac{(\partial_{\lambda} \Gamma)^2}{e^{2\Gamma} - 1}. \quad (\text{B3})$$

(ii) To calculate the fisher information associated with the measurement $\hat{\sigma}_{\perp}$, we rewrite $\hat{\sigma}_{\perp}$ as

$$\hat{\sigma}_{\perp} = \lim_{\psi \rightarrow \Phi} (\cos \psi \hat{\sigma}_y - \sin \psi \hat{\sigma}_x), \quad (\text{B4})$$

then obtain

$$\partial_{\lambda} \langle \hat{\sigma}_{\perp} \rangle = \lim_{\psi \rightarrow \Phi} \frac{\partial}{\partial \lambda} [e^{-\Gamma} (\cos \psi \sin \Phi - \sin \psi \cos \Phi)] = e^{-\Gamma} \partial_{\lambda} \Phi \quad (\text{B5})$$

Therefore, the fisher information associated with the measurement $\hat{\sigma}_{\perp}$ can be given as

$$\mathcal{F}_{\lambda}(\hat{\sigma}_{\perp}) = \frac{(\partial_{\lambda} \langle \hat{\sigma}_{\perp} \rangle)^2}{\langle \Delta \hat{\sigma}_{\perp}^2 \rangle} = e^{-2\Gamma} (\partial_{\lambda} \Phi)^2. \quad (\text{B6})$$

(iii) Now we calculate the the fisher information associated with the measurement $\hat{\Lambda} = \cos \varphi \hat{\sigma}_{\parallel} + \sin \varphi \hat{\sigma}_{\perp}$. The derivative of $\langle \hat{\Lambda} \rangle$ with respect to λ reads

$$\partial_{\lambda} \langle \hat{\Lambda} \rangle = \cos \varphi \partial_{\lambda} w + \sin \varphi w \partial_{\lambda} \Phi. \quad (\text{B7})$$

Then the fisher information reads

$$\mathcal{F}_{\lambda}(\hat{\Lambda}) = \frac{(\partial_{\lambda} \langle \hat{\Lambda} \rangle)^2}{\langle \Delta \hat{\Lambda}^2 \rangle} = \frac{w^2 \sin^2 \varphi (\partial_{\lambda} \Phi)^2 + \cos^2 \varphi (\partial_{\lambda} w)^2 + w \sin(2\varphi) (\partial_{\lambda} \Phi) (\partial_{\lambda} w)}{1 - w^2 \cos^2 \varphi}. \quad (\text{B8})$$

The QFI in Eq. (14) of the main text can be rewritten as

$$\mathcal{F}_{\lambda}^Q = \frac{(\partial_{\lambda} w)^2}{1 - w^2} + w^2 (\partial_{\lambda} \Phi)^2. \quad (\text{B9})$$

If $\hat{\Lambda}$ is the optimal measurement, it has to satisfy $\mathcal{F}_{\lambda}(\hat{\Lambda}) \equiv \mathcal{F}_{\lambda}^Q$, i.e.,

$$\frac{w^2 \sin^2 \varphi (\partial_{\lambda} \Phi)^2 + \cos^2 \varphi (\partial_{\lambda} w)^2 + w \sin(2\varphi) (\partial_{\lambda} \Phi) (\partial_{\lambda} w)}{1 - w^2 \cos^2 \varphi} \equiv \frac{(\partial_{\lambda} w)^2}{1 - w^2} + w^2 (\partial_{\lambda} \Phi)^2. \quad (\text{B10})$$

By simplifying the above equation, we obtain

$$a \tan^2 \varphi + b \tan \varphi + c = 0, \quad (\text{B11})$$

where $a = -\frac{(\partial_{\lambda} w)^2}{1 - w^2}$, $b = 2w \partial_{\lambda} \Phi \partial_{\lambda} w$ and $c = -(1 - w^2)w^2 (\partial_{\lambda} \Phi)^2$. By solving equation (B11), we obtain

$$\tan \varphi = \frac{w(1 - w^2) \partial_{\lambda} \Phi}{\partial_{\lambda} w}. \quad (\text{B12})$$

[1] H. P. Breuer and F. Petruccione, *The Theory of Open Quantum Systems* (Oxford University Press, Oxford, 2007).

[2] L. Viola, E. Knill, and S. Lloyd, *Dynamical Decoupling of*

Open Quantum Systems, Phys. Rev. Lett. 82, 2417 (1999).

[3] Q. S. Tan, Y. Huang, X. Yin, L. M. Kuang, and X. Wang, Enhancement of parameter estimation precision in noisy systems by dynamical decoupling pulses, Phys. Rev. A 87, 032102 (2013).

[4] J. I. Cirac, A. S. Parkins, R. Blatt, and P. Zoller, "Dark" squeezed states of the motion of a trapped ion Phys. Rev. Lett. 70, 556 (1993).

[5] J. F. Poyatos, J. I. Cirac, and P. Zoller, Quantum Reservoir Engineering with Laser Cooled Trapped Ions, Phys. Rev. Lett. 77, 4728 (1996).

[6] A. Recati, P.O. Fedichev, W. Zwerger, J. von Delft, and P. Zoller, Atomic Quantum Dots Coupled to a Reservoir of a Superfluid Bose-Einstein Condensate, Phys. Rev. Lett. 94, 040404 (2005).

[7] M. A. Cirone, G. De Chiara, G. M. Palma, and A. Recati, Collective decoherence of cold atoms coupled to a Bose-Einstein condensate, New J. Phys. 11, 103055 (2009).

[8] C. Benedetti, F. Buscemi, P. Bordone, and M. G. A. Paris, Quantum probes for the spectral properties of a classical environment, Phys. Rev. A 89, 032114 (2014).

[9] M. Bina, F. Grasselli, and M. G. A. Paris, Continuous-variable quantum probes for structured environments, Phys. Rev. A 97, 012125 (2018).

[10] M. Mehboudi, A. Lampo, C. Charalambous, L. A. Correa, M. Á. García-March, and M. Lewenstein, Using Polarons for sub-nK Quantum Nondemolition Thermometry in a Bose-Einstein Condensate, Phys. Rev. Lett. 122, 030403 (2019).

[11] D. Tamascelli, C. Benedetti, H. P. Breuer, and M. G. A. Paris, Quantum probing beyond pure dephasing, New Journal of Physics 22, 083027 (2020).

[12] W. Wu, S. Y. Bai, and J. H. An, Non-Markovian Sensing of a Quantum Reservoir, Phys. Rev. A 103, L010601 (2021).

[13] A. V. Kirkova, W. Li, and P. A. Ivanov, Adiabatic sensing technique for optimal temperature estimation using trapped ions, Phys. Rev. Research 3, 013244 (2021).

[14] D. Adam, Q. Bouton, J. Nettersheim, S. Burgardt, and A. Widera, Coherent and Dephasing Spectroscopy for Single-Impurity Probing of an Ultracold Bath, Phys. Rev. Lett. 129, 120404 (2022).

[15] M. M. Khan, M. Mehboudi, H. Terças, M. Lewenstein, and M. A. Garcia-March, Subnanokelvin thermometry of an interacting d -dimensional homogeneous Bose gas, Phys. Rev. Research 4, 023191 (2022).

[16] C. W. Helstrom, Quantum Detection and Estimation Theory (Academic, New York, 1976).

[17] A. S. Holevo, Probabilistic and Statistical Aspects of Quantum Theory (North-Holland, Amsterdam, 1982).

[18] W. Zhong, Z. Sun, J. Ma, X. G. Wang, and F. Nori, Fisherer information under decoherence in bloch representation, Phys. Rev. A 87, 022337 (2013).

[19] J. Liu, H. D. Yuan, X. M. Lu, and X. G. Wang, Quantum Fisherer information matrix and multiparameter estimation, Journal of Physics A: Mathematical and Theoretical 53, 023001 (2019).

[20] Y. M. Chu, Y. Liu, H. B. Liu, and J. M. Cai, Quantum Sensing with a Single-Qubit Pseudo-Hermitian System, Phys. Rev. Lett. 124, 020501 (2020).

[21] S. P. Wolski, D. Lachance-Quirion, Y. Tabuchi, S. Kono, A. Noguchi, K. Usami, and Y. Nakamura, Dissipation-Based Quantum Sensing of Magnons with a Superconducting Qubit, Phys. Rev. Lett. 125, 117701 (2020).

[22] S. Fernandez-Lorenzo and D. Porras, Quantum sensing close to a dissipative phase transition: Symmetry breaking and criticality as metrological resources, Phys. Rev. A 96, 013817 (2017).

[23] W. Wu and C. Shi, Quantum parameter estimation in a dissipative environment, Phys. Rev. A 102, 032607 (2020).

[24] F. Chapeau-Blondeau, Quantum parameter estimation on coherently superposed noisy channels, Phys. Rev. A 104, 032214 (2021).

[25] W. T. He, H. Y. Guang, Z. Y. Li, R. Q. Deng, N. N. Zhang, J. X. Zhao, F. G. Deng, and Q. Ai, Quantum metrology with one auxiliary particle in a correlated bath and its quantum simulation, Phys. Rev. A 104, 062429 (2021).

[26] J. H. Lu, W. Ning, X. Zhu, F. Wu, L. T. Shen, Z. B. Yang, and S. B. Zheng, Critical quantum sensing based on the Jaynes-Cummings model with a squeezing drive, Phys. Rev. A 106, 062616 (2022).

[27] L. Xu, J. B. Yuan, S. Q. Tang, W. Wu, Q. S. Tan, and L. M. Kuang, Non-Markovian enhanced temperature sensing in a dipolar Bose-Einstein condensate, Phys. Rev. A 108, 022608 (2023).

[28] K. Kakuyanagi, H. Toida, L. V. Abdurakhimov, and S. Saito, Submicrometer-scale temperature sensing using quantum coherence of a superconducting qubit, New Journal of Physics 25, 013036 (2023).

[29] A. J. Leggett, S. Chakravarty, A. T. Dorsey, Matthew P. A. Fisher, Anupam Garg, and W. Zwerger, Dynamics of the dissipative two-state system, Rev. Mod. Phys. 59, 1 (1987).

[30] M. T. Mitchison, T. Fogarty, G. Guarneri, S. Campbell, T. Busch, and J. Goold, In situ thermometry of a cold fermi gas via dephasing impurities, Phys. Rev. Lett. 125, 080402 (2020).

[31] S. Razavian, C. Benedetti, M. Bina, Y. Akbari-Kourbolagh, and M. G. A. Paris, Quantum thermometry by single-qubit dephasing, Eur. Phys. J. Plus 134, 284 (2019).

[32] F. Gebbia, C. Benedetti, F. Benatti, R. Floreanini, M. Bina, and M. G. A. Paris, Two-qubit quantum probes for the temperature of an ohmic environment, Phys. Rev. A 101, 032112 (2020).

[33] A. Candeloro and M. G. A. Paris, Discrimination of ohmic thermal baths by quantum dephasing probes, Phys. Rev. A 103, 012217 (2021).

[34] J. B. Yuan, B. Zhang, Y. J. Song, S. Q. Tang, X. W. Wang and L. M. Kuang, Quantum sensing of temperature close to absolute zero in a Bose-Einstein condensate, Phys. Rev. A 107, 063317 (2023).

[35] C. Benedetti, F. Salari Sehdaran, M. H. Zandi, and M. G. A. Paris, Quantum probes for the cutoff frequency of ohmic environments, Phys. Rev. A 97, 012126 (2018).

[36] F. S. Sehdaran, M. Bina, C. Benedetti, and M. G. A. Paris, Quantum probes for ohmic environments at thermal equilibrium, Entropy 21, 486 (2019).

[37] F. S. Sehdaran, M. H. Zandi, and A. Bahrampour, The effect of probe-ohmic environment coupling type and probe information of the cutoff frequency, Phys. Lett. A 383, 126006 (2019).

[38] Q. S. Tan, W. Wu, L. Xu, J. Liu, and L. M. Kuang, Quantum sensing of supersensitivity for the Ohmic quantum reservoir, Phys. Rev. A 106, 032602 (2022).

[39] H. Ather and A. Z. Chaudhry, Improving the estimation of environment parameters via initial probe-environment correlations, Phys. Rev. A 104, 012211 (2021).

[40] Q. S. Tan, J. B. Yuan, J. Q. Liao, and L. M. Kuang, Super-sensitive estimation of the coupling rate in cavity optomechanics with an impurity-doped Bose-Einstein condensate, Opt. Express 28, 22867 (2020).

[41] P. Haikka, S. McEndoo, G. De Chiara, G. M. Palma, and S. Maniscalco, Quantifying, characterizing, and controlling information flow in ultracold atomic gases, Phys. Rev. A 84, 031602(R) (2011).

[42] P. Haikka, S. McEndoo, and S. Maniscalco, Non-Markovian

probes in ultracold gases, *Phys. Rev. A* 87, 012127 (2013).

[43] J. B. Yuan, H. J. Xing, L. M. Kuang, and S. Yi, Quantum non-Markovian reservoirs of atomic condensates engineered via dipolar interactions, *Phys. Rev. A* 95, 033610 (2017)

[44] C. L. Degen, F. Reinhard, and P. Cappellaro, Quantum sensing, *Rev. Mod. Phys.* 89, 035002 (2017).

[45] I. Bloch, J. Dalibard, and W. Zwerger, Many-body physics with ultracold gases, *Rev. Mod. Phys.* 80, 885 (2008).

[46] C. Chin, R. Grimm, P. Julienne, and E. Tiesinga, Feshbach resonances in ultracold gases, *Rev. Mod. Phys.* 82, 1225 (2010).

[47] Y. J. Song and L. M. Kuang, Controlling Decoherence Speed Limit of a Single Impurity Atom in a Bose-Einstein-Condensate Reservoir, *Ann. Phys.* 531, 1800423 (2019).